Buckminsterfullerene fragments used as hydrogen carrier: Case of corannulene derivatives

Siham Naima Derrar[a,b*] and Ossama Rafai[c]

[a]Laboratoire de Structure, Elaboration et Application des Matériaux Moléculaires, Mostaganem University, Algeria
[b]Department of Pharmacy, Faculty of Medicine, Sidi Bel Abbès University, Algeria
[c]Faculty of Exact Sciences and Computer Science, Mostaganem University, Algeria

| CHRONICLE	ABSTRACT
	Buckminsterfullerene fragments are interesting to use in hydrogen adsorption because of the suitable properties possessed by their concave structure. In the present paper, adsorption of hydrogen on the bowl-shaped corannulene and its derivatives is investigated. Both electron donor and electron acceptor are explored in the substitution and 28 derivatives are generated. DFT calculations are performed by means of WB97XD functional. The substitution number and the substitution nature of corannulene derivatives are analyzed through results based on several parameters. Besides bowl depth and equilibrium distance, also charge distribution and some reactivity indices, based on MEDT, are reported. Results show that a newly created charge distribution contributes to a better binding process.

1. Introduction

Hydrogen is the most basic and abundant element in the universe, ranking first on the periodic table of all elements. Because hydrogen is the lightest element, it has the largest energy content in terms of weight but the lowest energy density in terms of volume of all the main fuels. The first-time hydrogen was used as an energy source was in the early 1820s. Hydrogen is a clean energy carrier; when it is burned in fuel cells, it produces heat and power or electricity without harming the environment or changing the climate[1]. As a result, it is a strong contender for use as an energy carrier in transportation systems such as cars and planes as well as in industry. Different ways for hydrogen production are to be cited[2]. It includes (a) from fossil fuels[3] where the hydrocarbons provide more than 90% of the traditional hydrogen manufacturing process-this can be reached through steam reforming, partial oxidation, autothermal oxidation and gasification[4-6]-, (b) through biomass and biological processes which includes thermochemical, pydrolysis and direct and indirect photo-biolysis[7-12] and (c) from solar energy, such as photovoltaics and bio-photolysis techniques.[13-15]

The use of hydrogen for mobility is now technically viable based on combustible batteries.[16] However, because hydrogen gas is extremely light, enormous tanks in vehicles are required to hold it. Hence, several compounds for rapid adsorption/desorption have been proposed to address this issue. Organometallic and inorganometallic complexes[17-19] and metal hydrides[20-22] have sparked a lot of attention, alongside carbon-based nanomaterials. Graphene sheets, nanotubes, and buckybowl systems are examples of the latter.[23-32] Among buckminsterfullerene fragments, corannulene has been widely investigated as a support for molecules and fragments and interesting intermolecular interactions properties have been reported.[33-40] In fact, corannulene ($C_{20}H_{10}$) is a buckybowl polyaromatic hydrocarbon. These materials feature concave (inside) and convex (outside) faces with non-equivalent electrostatic potentials and a non-symmetric charge distribution

throughout the molecular surface. Consequently, they exhibit a persistent dipole and possess distinct physical and chemical properties (**Fig. 1**).
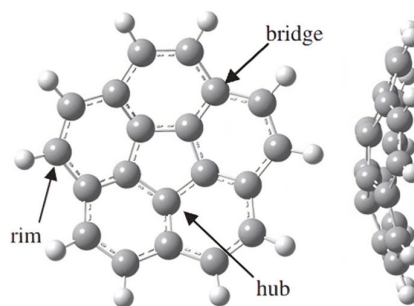
Fig. 1. Structure of corannulene molecule

In addition, decorating these molecules with suitable groups, such as compounds containing nitro groups, can lead to remarkable adsorption capacities. Indeed, these structures have recently garnered significant interest due to their fascinating properties, which are utilized in various applications and contexts.[41-43] Moreover, it is to be noted that by introducing NH_2 and NO_2 groups onto corannulene, the resulting functionalized derivatives can exhibit enhanced hydrogen adsorption properties. Indeed, The NH_2 group, being highly nucleophilic, provides active sites for hydrogen adsorption through strong hydrogen bonding interactions. Moreover, its ability to form stable intermediates with hydrogen molecules contributes to improved adsorption kinetics. Additionally, the presence of NH_2 groups introduces polar functionalities, enhancing the affinity towards hydrogen molecules. Similarly, the NO_2 group, known for its electron-withdrawing nature, offers favorable sites for hydrogen adsorption. The electronegative oxygen atoms in NO_2 group can engage in hydrogen bonding interactions, facilitating efficient hydrogen uptake. Furthermore, the electron-deficient nature of the NO_2 group enhances the polarization of hydrogen molecules, leading to stronger adsorption.

In the present paper, we look into the adsorption of hydrogen in various corannulene derivatives and we report the effect of two substituent groups, namely NH_2 and NO_2, on the energy of interaction with the dihydrogen molecule (H_2). We thus examine how an electron acceptor and an electron donor group contribute to hydrogen adsorption. In addition, we determine which group sites provide the best interaction energies.

2. Methodology

Full geometry optimization of all structures (with and without H_2) has been performed, without any symmetry constraints. Optimization has been established at WB97XD/6-31G level of theory, with default convergence criteria. This DFT functional[44] was chosen to account for the dispersion interactions that occur in corannulene derivatives and hydrogen. Since WB97XD functional performs suitably in non-bonded interactions and for the sake of calculation cost, it has been used instead of the MP2 method.

The orientation, chosen to evaluate interaction of H_2 with corannulene derivatives and to obtain the most stable adsorption position of each structure, is that where the hydrogen is oriented in the central pentagonal ring perpendicularly to the hub plan of corannulene (all along with z-axis), in the concavity of the corannulene molecule.

The pure corannulene molecule (pristine) is the first system model investigated in our systematic study. This latter is used as a benchmark for all types of comparisons. While the other systems studied result from the substitution of H atom, linked to the carbon in the "rim" position (**Fig. 1**). Two various substituent groups have been tested, namely NH_2 donor group and NO_2 acceptor group. This gives rise to 14 structures, for each substituent group (**Fig. 2** and **Fig. 3**), as it is illustrated in the following:

-Replacement of one peripheric H atom (mono- substitution) : Structure 1.
-Five structures dealing with the substitution of two peripheric H atoms (di-substitution): Structures 2-6.
-Eight structures concerning the substitution of three peripheric H atoms (tri-substitution): Structures 7-14.

Binding energies have been calculated by means of the following equation:

$$BE = E(Subst\text{-}cor + H_2) - [E(Subst\text{-}cor) + E(H_2)] \tag{1}$$

where $E(Subst\text{-}cor + H_2)$ is the energy of the substituted corannulene interacting with H_2, $E(Subst\text{-}cor)$ is the energy of the substituted corannulene, and $E(H_2)$ is the energy of the hydrogen molecule.

Basis set superposition error (BSSE) has been considered, by means of counterpoise corrections of Boys and Bernardi[45], via the following equation:

$$BE(CP) = BE + BSSE \tag{2}$$

where $BE(CP)$ is the BSSE-corrected binding energy, BE is the uncorrected binding energy, and BSSE is the counterpoise correction. All the calculations have been performed by Gaussian 09 program package.[46]
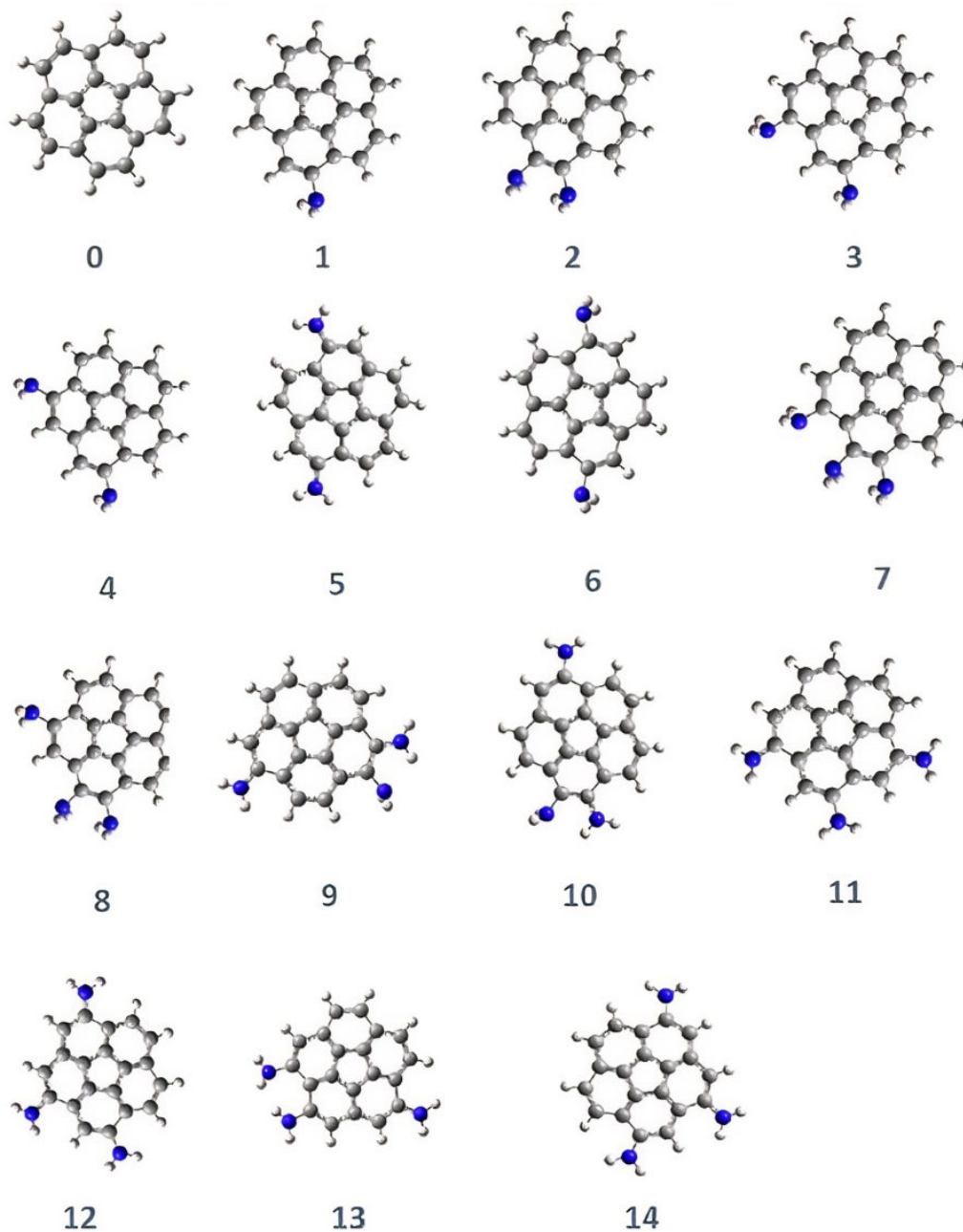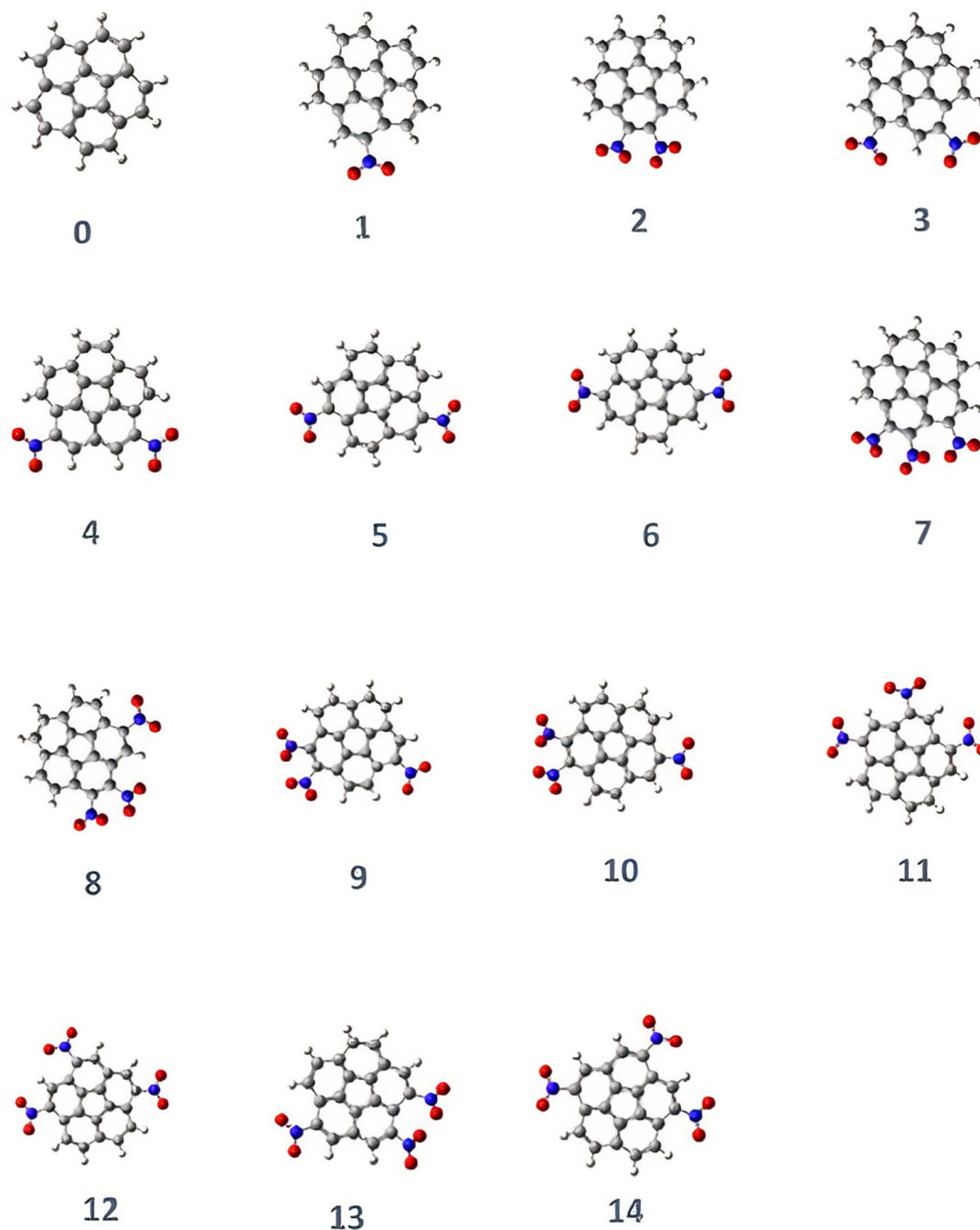

Fig. 2. Structures of pristine corannulene and NH_2-corannulene derivatives

Fig. 3: Structures of pristine corannulene and NO$_2$-corannulene derivatives

3. Results and discussion

3.1. Bowl depth

Since adsorption of hydrogen takes place in the concave side of the molecule, bowl depth value becomes an important parameter to analyze. It refers to the distance between the plan of the hub pentagon ring and the plan of the atom in rim position (**Fig. 1**). In our study we consider Nitrogen atom.   Compared to pristine, all the corannulene derivatives present deeper bowl depth, regardless the nature, the number, or the site of the substitution (**Tables 1** and **2**). It has also been shown that the presence of hydrogen, globally, increases the bowl depth values, for both substituents.

Table 1. Values of Bowl Depth (Å), Dipole Moment (μ, Debye), Relative Energy (ΔE, kcal/mol), Equilibrium Distance (Eq. distance, Å), Binding Energy (BE, kcal/mol), Parallel (P) or Horizontal (H) position of H_2 for pristine and NH_2-substituted corannulene, with and without H_2

		Without H_2		With H_2					
Label	Molecule	Bowl depth	μ	Bowl depth	ΔE	μ	Eq. distance	BE	Position of H_2
0	Pristine	4.636	2.2	4.658	–	2.3	2.585	-2.403	P
1	Cor-NH_2	4.914	3.4	4.932	–	3.4	2.532	-2.446	H
2	Cor-NH_2(1-2)	4.941	3.2	4.959	3.765	3.2	2.532	-2.490	P
3	Cor-NH_2(1-3)	4.918	4.5	4.936	0.607	4.5	2.772	-2.830	H
4	Cor-NH_2(1-4)	4.926	3.2	4.944	0.000	3.2	2.532	-2.465	P
5	Cor-NH_2(1-5)	4.943	3.0	4.961	0.000	3.0	2.551	-2.465	P
6	Cor-NH_2(1-6)	4.955	2.8	4.973	1.255	2.8	2.528	-2.477	P
7	Cor-NH_2(1-2-3)	4.920	5.7	4.938	3.137	5.7	2.569	-2.452	P
8	Cor-NH_2(1-2-4)	4.940	3.7	4.959	2.510	3.70	2.577	-2.458	P
9	Cor-NH_2(1-2-5)	4.961	3.5	4.979	3.137	3.5	2.566	-2.496	P
10	Cor-NH_2(1-2-6)	4.977	2.7	4.996	3.765	2.7	2.559	-2.490	P
11	Cor-NH_2(1-3-5)	4.937	4.6	4.965	0.627	4.6	2.567	-2.483	P
12	Cor-NH_2(1-3-6)	4.954	3.2	4.972	1.255	3.2	2.561	-2.477	P
13	Cor-NH_2(1-4-5)	4.939	3.2	4.957	0.000	3.2	2.570	-2.452	P
14	Cor-NH_2(1-4-6)	4.954	3.2	4.972	1.255	3.2	2.562	-2.477	P

Table 2. Values of Bowl Depth (Å), Dipole Moment (μ, Debye), Relative Energy (ΔE, kcal/mol), Equilibrium Distance (Eq. distance, Å, Binding Energy (BE, kcal/mol), Parallel (P) or Horizontal (H) position of H_2 for pristine and NO_2-substituted corannulene, with and without H_2

		Without H_2		With H_2					
Label	Molecule	Bowl depth	μ	Bowl depth	ΔE	μ	Eq. distance	BE	Position of H_2
0	Pristine	4.636	2.2	4.658	–	2.3	2.585	-2.403	P
1	Cor-NO_2	4.947	6.0	4.781	–	6.0	2.569	-2.408	P
2	Cor-NO_2(1-2)	4.933	9.2	4.957	13.805	9.2	2.854	-2.709	H
3	Cor-NO_2(1-3)	4.945	9.2	4.994	0.627	9.2	2.849	-2.640	H
4	Cor-NO_2(1-4)	4.966	5.6	4.982	0.627	5.6	2.950	-2.428	H
5	Cor-NO_2(1-5)	5.000	3.6	4.664	0.000	3.6	2.574	-2.308	P
6	Cor-NO_2(1-6)	5.032	1.3	5.053	0.627	1.3	2.576	-2.333	P
7	Cor-NO_2(1-2-3)	4.957	12.9	4.978	18.825	12.8	2.875	-2.703	H
8	Cor-NO_2(1-2-4)	4.956	9.9	–	–	–	–	–	–
9	Cor-NO_2(1-2-5)	4.988	8.00	5.007	11.295	7.9	2.854	-2.703	H
10	Cor-NO_2(1-2-6)	5.026	3.8	5.045	11.922	3.8	2.573	-2.327	P
11	Cor-NO_2(1-3-5)	4.977	8.9	4.997	0.000	8.9	2.586	-2.270	P
12	Cor-NO_2(1-3-6)	5.011	4.5	5.031	0.000	4.5	2.579	-2.283	P
13	Cor-NO_2(1-4-5)	4.976	7.7	4.998	7.530	7.7	2.605	-2.258	P
14	Cor-NO_2(1-4-6)	5.011	4.5	5.031	0.000	4.5	2.855	-2.659	H

3.2. Equilibrium distance

Tables 1 and **Table 2** gather the final positions of hydrogen, after a full geometry optimization of the complexes studied. The equilibrium distance refers to the distance between the plan of the central five-membered cycle and the nearest hydrogen atom in H_2. Two cases have been registered, after the full geometry optimization, as mentioned in the above mentioned tables:

- Hydrogen molecule remains perpendicular to the carrier molecule. The smallest equilibrium distance is attributed to pristine corannulene, for both substituent groups.
- Hydrogen molecule takes a horizontal position. This occurs mainly for NO_2 –substituted structures. It can be explained by the attraction of oxygen atoms exerted on hydrogen. This generates longer equilibrium distances in the substituted systems, compared to pristine.

The largest equilibrium distance values are recorded in NO_2 –substituted structures. In addition, within the same substitution number, and for both groups, the horizontal position of H_2 appears to strengthen and to enhance the hydrogen-system interaction. Average H…H distances are 0.7422 Å and 0.7430 Å for systems with perpendicular and parallel H_2 positions, respectively.

3.3. Energy aspects

Relative energy values, corresponding to the studied H_2-systems (**Fig. 2** and **Fig. 3**), are collected in **Tables 1** and **2**. Results reveal that the most stable NH_2 derivatives are the di-substituted (1-4) and (1-5) in addition to the tri-substituted (1-

4-5). Concomitantly, systems (corannulene-NO$_2$-1-5) besides to (corannulene-NO$_2$-1-3-5), (corannulene-NO$_2$-1-3-6) and (corannulene-NO$_2$-1-4-6) exhibit the least stability. Results also show some isoenergetic systems, explicitly, NO$_2$-di-substituted corannulene (1-3), (1-4) and (1-6).

3.4. Binding energy

Binding energy values, calculated upon Eq. (1), are listed in **Tables 1** and **2**. Results highlight a physisorption phenomenon for all the systems studied. Doping pristine corannulene leads to higher binding energies in all the NH$_2$ derivatives and in only some of them in NO$_2$ derivatives (**Table 1**).

If one looks carefully to **Tables 1** and **2** and to **Fig. 4**, it seems that the horizontal position of H$_2$ favors its adsorption. In fact, results show that structures with significant BE values are attributed to those with parallel hydrogen position. This is probably since there are two sites interacting with the host system, in parallel position, rather than only one in perpendicular position. Hence, the position of H$_2$ plays a key role in the adsorption process.

For the same position of H$_2$, a comparison between NO$_2$ and NH$_2$ groups can be established for (1-3)-disubstituted corannulene. It reveals a better binding in favor of NO$_2$ group. Hence, NO$_2$ acceptor group seems to create a new charge distribution, more suitable for enhancing interaction than with NH$_2$ donor group.

a)

b)
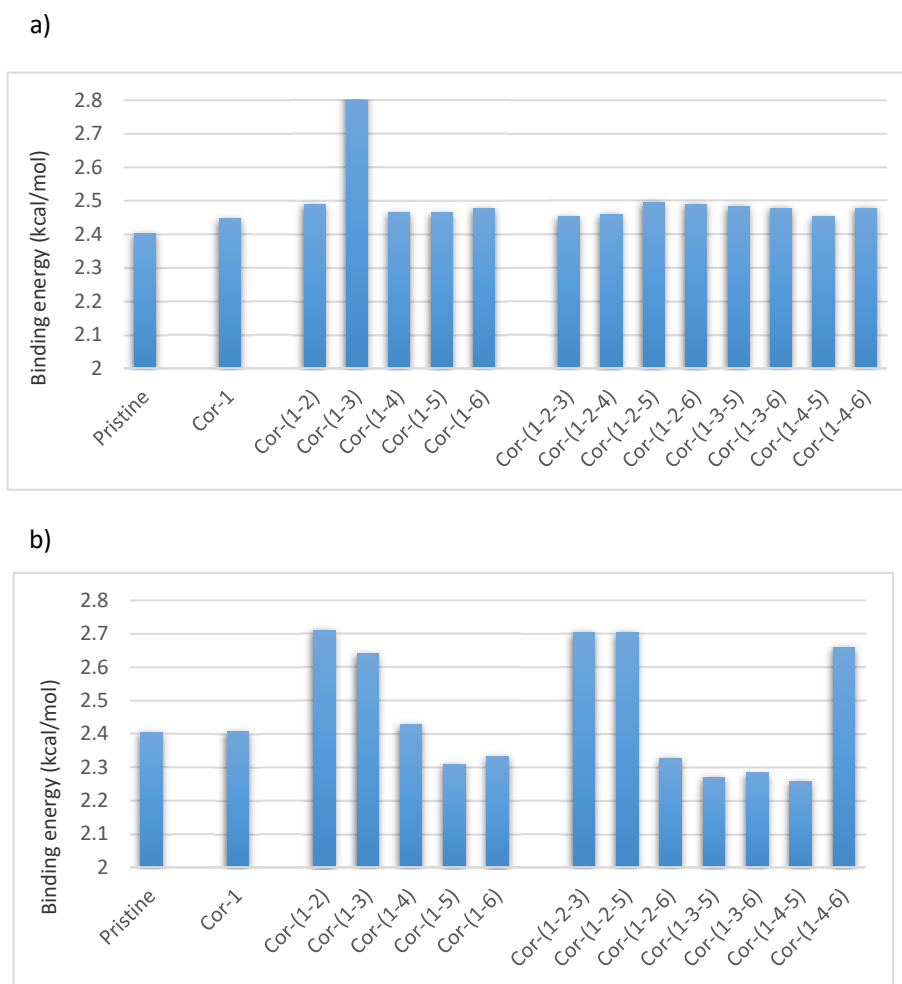
Fig. 4. Evolution of binding energy *versus* substitution of corannulene with: a) NH$_2$ and b) NO$_2$

3.5. Dipole moment

Dipole moment represents, in such a kind of buckybowl molecules, a key tool since it is generated from the charge distribution created within the substituted systems. Results, resumed in **Table 1** and **Table 2**, indicate that doping, with NH$_2$ and NO$_2$, enhances dipole moment values. On the other hand, the addition of hydrogen to corannulene derivatives has two,

completely different, impacts on dipole moment, for each substituent. In fact, hydrogen adsorption increases dipole moment values for NH_2-doped systems while it decreases it for NO_2-doped ones. It is noticed that among the largest dipole moment values correspond the highest binding energy amounts.

3.6. MEDT reactivity indices

In this part, some Molecular Electron Density reactivity indices of molecules, in their ground state, have been treated to evaluate their reactivity.[47] In fact, electronic chemical potential μ has been calculated and mentioned in **Table 3** and **Table 4**. Results show greater potential values for systems with NH_2 group indicating their high capability to exchange electron density with the environment.

Calculated chemical hardness η determines the resistance to exchange electronic density with the environment. The chemical softness S is expressed as the inverse of hardness. The reported values have been found in the same range for all the systems studied.

The electrophilicity index ω encompasses the tendency of an electrophile to acquire an extra amount of electron density. Taking a closer look at **Table 3** and **Table 4,** it seems that electrophilicity enhances with substitution number, for NO_2 derivatives. According to the scale established to classify organic molecules upon their electrophilicity values, it seems that NO_2-susbtituted corannulene systems are strong electrophiles (ω > 1.5).

Table 3. Values of Electronic Chemical Potential (μ, eV), Chemical hardness (η, eV), Chemical softness (S, eV) and Electrophilicity (ω, eV), for pristine and NH_2-substituted corannulene, with H_2

Label	Molecule	μ (potential)	η	S	ω
0	Pristine	-3.945	4.068	0.245	1.913
1	Cor-NH₂	-3.346	3.591	0.278	1.559
2	Cor-NH₂(1-2)	-3.211	3.469	0.288	1.486
3	Cor-NH₂(1-3)	-3.047	3.537	0.282	1.312
4	Cor-NH₂(1-4)	-3.129	3.578	0.279	1.368
5	Cor-NH₂(1-5)	-3.184	3.578	0.279	1.417
6	Cor-NH₂(1-6)	-3.020	3.387	0.295	1.346
7	Cor-NH₂(1-2-3)	-2.911	3.455	0.289	1.226
8	Cor-NH₂(1-2-4)	-2.993	3.523	0.283	1.271
9	Cor-NH₂(1-2-5)	-3.075	3.496	0.286	1.352
10	Cor-NH₂(1-2-6)	-2.938	3.306	0.302	1.305
11	Cor-NH₂(1-3-5)	-2.857	3.537	0.283	1.154
12	Cor-NH₂(1-3-6)	-2.803	3.401	0.294	1.155
13	Cor-NH₂(1-4-5)	-2.993	3.564	0.280	1.257
14	Cor-NH₂(1-4-6)	-2.803	3.401	0.294	1.155

Table 4. Values of Electronic Chemical Potential (μ, eV), Chemical hardness (η, eV), Chemical softness (S, eV) and Electrophilicity (ω, eV) for pristine and NO_2-substituted corannulene, with H_2

Label	Molecule	μ (potential)	η	S	ω
0	Pristine	-3.945	4.068	0.245	1.913
1	Cor-NO₂	-4.870	3.591	0.278	3.302
2	Cor-NO₂(1-2)	-5.306	3.523	0.284	3.996
3	Cor-NO₂(1-3)	-5.333	3.523	0.284	4.036
4	Cor-NO₂(1-4)	-5.360	3.551	0.282	4.045
5	Cor-NO₂(1-5)	-5.387	3.578	0.279	4.055
6	Cor-NO₂(1-6)	-5.442	3.496	0.286	4.236
7	Cor-NO₂(1-2-3)	-5.659	3.591	0.278	4.459
8	Cor-NO₂(1-2-4)	−	−	−	−
9	Cor-NO₂(1-2-5)	-5.769	3.578	0.279	4.651
10	Cor-NO₂(1-2-6)	-5.823	3.483	0.287	4.867
11	Cor-NO₂(1-3-5)	-5.796	3.591	0.278	4.677
12	Cor-NO₂(1-3-6)	-5.877	3.483	0.287	4.958
13	Cor-NO₂(1-4-5)	-5.714	3.619	0.276	4.511
14	Cor-NO₂(1-4-6)	-5.877	3.496	0.286	4.939

3.7. Charge distribution

Natural population analysis (NPA) has been investigated and the related values have been summarized in **Table 5**. Results show that doping corannulene with NH_2 and NO_2 substituents leads to a new charge distribution within the systems.

Hub plan gets less charged in decorated corannulene than in pristine. Indeed, the charge of this plan is directly influenced by the substituent nature since it has been globally found more pronounced for NO_2 group.

It also has been noticed that the substituent number exerts some effects on hub plan charge. Actually, the hub plan charge values increase with the progression of substitution number for NH_2, opposite to what is recorded for NO_2.

On the other hand, as shown in **Table 5**, the interaction of the systems with hydrogen increases the hub plan charge magnitudes for NH_2 substituent and decreases it for NO_2.

Charge magnitudes also show that the addition of hydrogen reacts more on hub plan than on substituents. Moreover, hydrogen highly affects the hub plan charge when no substituents exist. Charge recorded on hydrogen remains the highest for pristine corannulene.

Table 5. NPA charges (e) of pristine and corannulene derivatives with and without H_2

Structure	Without H_2		With H_2		
	Hub plan	Substituent	Hub plan	Substituent	H_2
Pristine	-0.070		-0.080		-0.013
NH$_2$					
Cor-1	-0.008	-0.012	-0.008	-0.011	-0.001
Cor-1-2	-0.008	-0.127/0.001	-0.009	-0.127/0.002	-0.002
Cor-1-2-3	-0.098	-0.001/ -0.141/-0.020	-0.106	-0.001/ -0.139/-0.020	-0.001
NO$_2$					
Cor-1	-0.058	-0.287	-0.044	-0.286	-0.002
Cor-1-2	-0.034	-0.222/-0.213	-0.032	-0.222/-0.213	-0.002
Cor-1-2-3	-0.023	-0.218/ -0.177/-0.247	-0.012	-0.210/ -0.180/-0.241	-0.001

The trend of the calculated charges and the electrophilicity (**Tables 3** and **4**) seems to corroborate. In fact, decorating corannulene with electrophilic and nucleophilic groups plays a role in the density charge of the hub plan (if one compares with pristine). The more a substituent is added, the more the charge is augmented or diminished which can have a direct impact on reactivity and hence on binding energy.

4. Conclusion

Adsorption of hydrogen on 28 substituted corannulene systems has been carried out using WB97XD functional. Both electron donor and electron acceptor have been tested. Results revealed, after a full geometry optimization, that hydrogen can be adsorbed, either in a perpendicular or a horizontal position, towards the carrier molecule. In addition, the presence of hydrogen tends to increase the bowl depth magnitude. On the other hand, hydrogen adsorption increases dipole moment values for NH_2-doped systems while it decreases it for NO_2-doped ones. Based on the results recorded for pristine corannulene, a new charge distribution appears in the substituted systems. Besides, the presence of hydrogen reacts mainly on the charge of the hub plan of corannulene doped systems. In terms of binding energy, it can be stated that hydrogen adsorption seems to be governed by the position of the hydrogen molecule. Horizontal hydrogen position is revealed as the best one as it creates two interaction sites within the complex. When comparison is allowed, a preference appears in favor of NO_2 group, due to a newly created charge distribution which contributes to a better binding process.
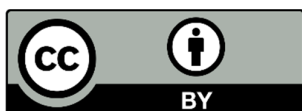
References

1. Ghiasi R. and Valizadeh A. (**2021**) Hydrogen adsorption and storage on palladium-functionalized graphyne and its boron nitride analogue. *J. Struct. Chem.*, 62, 835-844.
2. Abadalla A. M., Hossain S., Nisfindy O. B., Azad T., Dawood M. and Azad K. (**2018**) Hydrogen production, storage, transportation and key challenges with applications: A review. *Energy Convers. and Manage.*, 165, 602-627.
3. Peraldo Bicelli L. (**1986**) Hydrogen: A clean energy source. *Int. J. Hydrog. Energy*, 11(9), 555-562.
4. Acar C. and Dincer I. (**2014**) Comparative assessment of hydrogen production methods from renewable and non-renewable sources. *Int. J. Hydrog. Energy*, 39(1), 1-12.
5. Adris A. M., Pruden B., Lim, C. J. and Grace J. (**1993**) On the reported attempts to radically improve the performance of the steam methane reforming reactor. *Can. J. Chem. Eng.*, 74(2), 177-186.
6. Krumpelt M., Krause T. R., Carter J. D., Kopasz J. P. and Ahmed S. (**2002**) Fuel processing for fuel cell systems in transportation and portable power applications. *Catal. Today*, 77, 3-16.
7. Demirbaş A. (**2001**) Biomass resource facilities and biomass conversion processing for fuels and chemicals. *Energy Convers. and Manage.*, 42(11), 1357-1378.
8. Liu S., Zhu J., Chen M., Xin W., Yang Z. and Kong L. (**2014**) Hydrogen production via catalytic pyrolysis of biomass in a two-stage fixed bed reactor system. *Int. J. Hydrog. Energy*, 39(25), 13128-13135.
9. Rabah M. A. and Eldighidy S. M. (**1989**) Low cost hydrogen production from waste. *Int. J. Hydrog. Energy*, 14(4), 221-227.

10. Levin D. B., Pitt L., and Love M. (**2004**) Biohydrogen production: prospects and limitations to practical application. *Int. J. Hydrog. Energy*, 29(2), 173-185.

11. Ni M., Leung D. Y. C., Leung M. K. H. and Sumathy K. (**2006**) An overview of hydrogen production from biomass. *Fuel Process. Technol.*, 87, 461-472.

12. Lin C. Y. and Jo C. H. (**2003**) Hydrogen production from sucrose using an anaerobic sequencing batch reactor process. *J. Chem. Technol. Biotechnol.*, 78(6), 678-684.

13. Ozcan H and Dincer I. (**2014**) Energy and exergy analyses of a solar driven Mg-Cl hybrid thermochemical cycle for co-production of power and hydrogen. *Int. J. Hydrog. Energy*, 39 (28), 15330-15341.

14. Zeng K. and Zhang D. Recent progress in alkaline water electrolysis for hydrogen production and applications. *Prog. Energy Combust. Sci.*, 36(3), 307-326.

15. Dincer I. (**2010**) Green methods for hydrogen production. *Int. J. Hydrog. Energy* 2012, 37(2), 1954-1971. https://doi.org/10.1016/j.ijhydene.2011.03.173.

16. Bethoux O. (**2020**) Hydrogen Fuel Cell Road Vehicles: State of the Art and Perspectives. *Energies*, 13, 5843.

17. Xia L., Liu Q., Wang F. and Lu J. (**2016**) Improving the hydrogen storage properties of metal-organic framework by functionalization. *J. Mol. Model.*, 22(10), 254.

18. Petrushenko I. K. and Bettinger H. F. (**2001**) Hydrogen adsorption on inorganic benzenes decorated with alkali metal cations: theoretical study. *Phys. Chem. Chem. Phys.*, 23, 5315-5324.

19. Railey P., Song Y., Liu T. and Li Y. (**2017**) Metal organic frameworks with immobilized nanoparticles: Synthesis and applications in photocatalytic hydrogen generation and energy storage. *Mater. Res. Bull.*, 96, 385-394.

20. Zuettel A. (**2003**) Materials for hydrogen storage. *Mater. Today*, 6(9), 24–33.

21. Grochala W. and Edwards P. P. (**2004**) Thermal decomposition of the non-interstitial hydrides for the storage and production of hydrogen. *Chem. Rev.*, 104, 1283–1316.

22. Sakintuna B., Lamari-Darkrim F. and Hirscher M. (**2007**) Metal hydride materials for solid hydrogen storage: a review. *Int. J. Hydrog. Energy*, 32, 1121-1140.

23. Darkrim F. L., Malbrunot P. and Tartaglia G. P. (**2002**) Review of hydrogen storage by adsorption in carbon nanotubes. *Int. J. Hydrog. Energy*, 27, 193-202.

24. Dillon A. C. and Heben M. J. (**2001**) Hydrogen storage using carbon adsorbents: past, present and future. *Appl. Phys. A Mater. Sci. Process*, 72(2), 133-142.

25. Ye Y., Ahn C. C., Witham C., Fultz B., Liu J., Rinzler A. G. and Smalley R. E. (**1999**) Hydrogen adsorption and cohesive energy of single-walled carbon nanotubes. *Appl. Phys. Lett.*, 74, 2307-2309.

26. Moradi M. and Naderi N. (**2014**) First principle study of hydrogen storage on the graphene-like aluminum nitride nanosheet. *Struct. Chem.*, 25, 1289–1296.

27. Jiang H., Cheng X. L., Zhang H., Tang Y. J. and Wang J. (**2015**) J. Molecular dynamic investigations of hydrogen storage efficiency of graphene sheets with the bubble structure. *Struct. Chem.*, 26, 531–537.

28. Dillon A. C., Jones K. M., Bekkedahl T. A., Kiang C. H., Bethune D. S. and Heben M. J. (**1997**) Storage of hydrogen in single-walled carbon nanotubes. *Nature*, 386(6623), 377-379.

29. Armaković S., Armaković S. J., Šetrajčić J. P. and Dzambas L. D. (**2013**) Specificities of boron disubstituted sumanenes. *J. Mol. Model.*, 19, 1153–1166.

30. Reisi-Vanani A. and Shamsali F. (**2017**) Influence of nitrogen doping in sumanene framework toward hydrogen storage: a computational study. *J. Mol. Graphics and Modeling*, 76, 475–487.

31. Derrar S. N. and Belhakem M. (**2017**) Heterosubstituted sumanene as media for hydrogen storage: a theoretical study. *Int. J. Hydrog. Energy*, 42, 19583–19590.

32. Derrar S. N. (**2021**) Study of hydrogen adsorption by N+ - and Si-decorated sumanene. *Struct. Chem.*, 32, 759–765.

33. Gaboardi M., Pratt F., Milanese C., Taylor J., Siegel J. and Fernandez Alonso F. (**2019**) The interaction of hydrogen with corannulene, a promising new platform for energy storage. *Carbon*, 155, 432–437.

34. Rellán-Piñeiro M., Rodríguez-Otero J., Cabaleiro-Lago E. M. and Josa D. (**2013**) DFT and MP2 study of the interaction between corannulene and alkali cations. *J. Mol. Model.*, 19, 2049–2055.

35. Reisi-Vanani A. and Faghih S. (**2014**) Computational study of the molecular hydrogen physisorption in some of the corannulene derivatives as a carbon nanostructure. *J. Saudi. Chem. Society*, 18(5), 666-673.

36. Perez C., Steber A. L., Rijs A. M., Temelso B., Shields G. C., Lopez J. C., Kisiel Z. and Schnell M. (**2017**) Corannulene and its complex with water: A tiny cup of water. *Phys. Chem. Chem. Phys.*, 19, 14214-14223.

37. Josa D., Rodríguez-Otero J., Cabaleiro-Lago E. M., Santos L. A. and Ramalho T. C. (**2014**) Substituted Corannulenes and Sumanenes as Fullerene Receptors. A DFT-D Study. *J. Phys. Chem. A*, 118(40), 9521-9528.

38. Reisi-Vanani A., Rahimi S., Nasiri Kokhdan S. and Ebrahimpour-Komleh H. (**2015**) Computational study of the gas phase reaction of hydrogen azide and corannulene: a DFT study. *Comput. and Theoret. Chem.*, 1070, 94-101.

39. Banerjee S., Pillai C. G. S. and Majumdar C. (**2011**) Hydrogen absorption behaviour of doped corannulene: A first principles study. *Int. J. Hydrog. Energy*, 36(8), 4976-4983.

40. Chen X., Bai F. Q., Tang Y. and Zhang H. X. (**2016**) How the substituents in corannulene and sumanene derivatives alter their molecular assemblings and charge transport properties? —A theoretical study with a dimer model. *J. of Comput. Chem.*, 37(9), 813-824.

41. Sadowski M, Synkiewicz-Musialska B and Kula K. (**2024**) (1E,3E)-1,4-dinitro-1,3-butadiene—synthesis, spectral characteristics and computational study based on MEDT, ADME and PASS simulation. *Molecules*, 29, 542.

42. Ballini R., Petrini M. and Rosini G. (**2008**) Nitroalkanes as central reagents in the synthesis of spiroketals. *Molecules*, 13, 319-330.

43. Nishiwaki N. (**2020**) Walk through recent nitro chemistry advances. *Molecules*, 25, 3680.

44. Chai J. D. and Head-Gordon M. (**2008**) Long-range corrected hybrid density functionals with damped atom-atom dispersion corrections. *Phys. Chem. Chem. Phys.*, 10, 6615-6620.

45. Boys S. F. and Bernardi F. D. (**1970**) The calculation of small molecular interactions by the differences of separate total energies. Some procedures with reduced errors. *Mol. Phys.*, 19, 553–566.

46. Gaussian 09, Revision A.02, Frisch, M.-J.; Trucks, G.-W.; Schlegel, H.-B.; Scuseria, G.-E.; Robb, M.-A.; Cheeseman, J.-R.; Scalmani, G.; Barone, V.; Petersson, G.-A.; Nakatsuji, H.; Li, X.; Caricato, M.; Marenich, M.; Bloino, J.; Janesko, B.-J.; Gomperts, R.; Mennucci, B.; Hratchian, H.-P.; Ortiz, J.-V.; Izmaylov, A.-F.; Sonnenberg, J.-L.; Williams-Young, D.; Ding, F.; Lipparini, F.; Egidi, F.; Goings, J.; Peng, B.; Petrone, A.; Henderson, T.; Ranasinghe, D.; Zakrzewski, V.-G.; Gao, J.; Rega, N.; Zheng, G.; Liang, W.; Hada, M.; Ehara, M.; Toyota, K.; Fukuda, R.; Hasegawa, J.; Ishida, M.; Nakajima, T.; Honda, Y.; Kitao, O.; Nakai, H.; Vreven, T.; Throssell, K.; Montgomery Jr., J.-A, , Peralta, J.-E.; Ogliaro, F.; Bearpark, M.; Heyd, J.-J.; Brothers, E.; Kudin, K.-N.; Staroverov, V.-N.; Keith, T.; Kobayashi, R.; Normand, J.; Raghavachari, K.; Rendell, A.; Burant, J.-C.; Iyengar, S.-S.; Tomasi, J.; Cossi, M.; Millam, J.-M.; Klene, M.; Adamo, C.; Cammi, R.; Ochterski, J.-W.; Martin, R.-L.; Morokuma, K.; Farkas, O.; Foresman, J.-B.; Fox, D.-J. (**2016**) Gaussian, Inc., Wallingford CT

47. Domingo L. R., Ríos-Gutiérrez M. and Pérez P. (**2016**) Applications of the Conceptual Density Functional Theory Indices to Organic Chemistry Reactivity. Molecules, 21, 748.